OVERVIEW OF FIELD AND LABORATORY STUDIES OF UNSATURATED ZONE MATRIX DIFFUSION AND RELATED FRACTURE–MATRIX INTERACTIONS

Prepared for

U.S. Nuclear Regulatory Commission
Contract NRC–02–07–006

Prepared by

Jude McMurry

Center for Nuclear Waste Regulatory Analyses
San Antonio, Texas

October 2007

CONTENTS

FIGURE

TABLE

ACKNOWLEDGMENTS

This report was prepared to document work performed by the Center for Nuclear Waste Regulatory Analyses (CNWRA) for the U.S. Nuclear Regulatory Commission (NRC) under Contract No. NRC–02–07–006. The activities reported here were performed on behalf of the NRC Office of Nuclear Material Safety and Safeguards, Division of High-Level Waste Repository Safety. This report is an independent product of CNWRA and does not necessarily reflect the view or regulatory position of NRC.

The author gratefully acknowledges W. Murphy, R. Fedors, and J. Winterle for helpful discussions of this topic. Technical reviewer J. Winterle, programmatic reviewer B. Sagar, and editorial reviewer L. Mulverhill are thanked for their improvements. Appreciation is due to D. Waiting and L. Naukam for assistance in the preparation of this report.

QUALITY OF DATA, ANALYSES, AND CODE DEVELOPMENT

DATA: No original CNWRA data or analyses were generated for this report.

ANALYSES AND CODES: This report is a summary of previously published research taken from the open literature. The data and analytical results presented here are documented in the referenced studies, which should be consulted for additional information about the qualification of the analyses and the computer codes that were used to generate the simulations. No original calculations or analyses were performed for this report.

1 INTRODUCTION

The aqueous transport of radionuclides from a geologic repository can be affected by groundwater flow paths, by concentrations of radionuclides released from the repository as dissolved species or as particulates (including colloids), and by the sorptive capacity of the rocks and sediments through which the radionuclides travel. In fractured rocks, another factor to consider is fracture–matrix interactions, by which the transport of dissolved radionuclides can be delayed by transfer from flowing groundwater in the fractures to the relatively slower moving water in the rock matrix. Fracture–matrix interactions also increase the potential for retardation of certain radionuclides by sorption in the matrix because the rock matrix has a much larger total surface area than fractures.

Even where there is a strong permeability contrast between fractures and the matrix, such that water tends to remain in the fracture flow path, contaminants can move between the fracture and the matrix by the process of matrix diffusion: the net movement of a substance from an area of high concentration (e.g., in the water in the fracture) to an area of low concentration (in water in the matrix). The matrix diffusion rate is influenced not only by the molecular (free water) diffusion rate of a particular contaminant and by the properties of the solution but also by properties of the rock matrix through which the diffusion occurs (e.g., size and distribution of the pore openings and the tortuousity of the path through the rock). Fracture–matrix interactions in unsaturated rocks may also be influenced by advection, including movement from fracture to matrix in response to capillary forces, and by the number of fractures that are active (flowing). Mechanical dispersion and diffusion along flow paths further complicate the interpretation of radionuclide transport studies in natural fracture systems.

Performance assessment studies for proposed geological repositories in saturated rocks in Sweden, Finland, and Switzerland have represented matrix diffusion in transport models as an important retardation process, but conservative assumptions are applied in these models to compensate for uncertainties about heterogeneous flow systems in fractured, low-permeability rocks (Jakob, 2004). Fracture–matrix interactions in unsaturated rocks are not as well characterized or constrained by tracer experiments as they are in saturated rocks. In Bechtel SAIC Company, LLC (2003), the U.S. Department of Energy (DOE) identified matrix diffusion in its performance assessment model at Yucca Mountain in southern Nevada as an important natural barrier to radionuclide transport in the unsaturated zone beneath a potential repository. Given uncertainties about the effectiveness of matrix diffusion as well as other processes that affect fracture–matrix interactions in unsaturated flow regimes, the U.S. Nuclear Regulatory Commission (NRC) performance assessment model for Yucca Mountain conservatively assumes that there is no exchange between matrix and fractures in the unsaturated zone. This is a simplifying bounding assumption for modeling purposes; clearly, the physics of contaminant transport in a fracture–matrix system would dictate that some degree of fracture–matrix interaction is likely to occur. The question, however, is how much credit for this process can reasonably be taken in the absence of quantifiable measurements or unambiguous interpretation of drift-scale experimental data. Several of the key technical issue agreement items between DOE and NRC (NRC, 2007) deal with questions related to DOE support for unsaturated zone flow and transport processes, including matrix diffusion and implementation of the active fracture model, at Yucca Mountain.

This report provides an overview of current published research that describes field and laboratory studies of matrix diffusion and other examples of fracture–matrix interaction in unsaturated flow regimes, particularly in terms of pertinent DOE field experiments at Yucca Mountain. In addition to the relatively few studies that have explicitly investigated unsaturated zone matrix diffusion, the report summarizes other field and laboratory studies that have documented related unsaturated zone flow and transport processes.

2 YUCCA MOUNTAIN FIELD AND LABORATORY STUDIES

Compared to studies of matrix diffusion in saturated rocks, there have been few well-constrained field experiments that explicitly investigated matrix diffusion as a transport process in unsaturated rocks. The field experiments that are most directly relevant to matrix diffusion in a potential repository at Yucca Mountain are those that have been conducted at or near the site itself. Of these experiments, DOE field tests in welded tuffs in the Exploratory Studies Facility at Alcove 8–Niche 3, Alcove 6, and Alcove 1 have provided data that DOE interpreted to indicate that tracer migration was delayed in some cases by matrix diffusion. Several other field tests, briefly described here, have investigated the relationships between infiltration, seepage, fracture flow, preferential flow pathways, and imbibition in welded and nonwelded tuffs at and near Yucca Mountain. Insights from these studies are closely related to matrix diffusion studies because all of the processes influence the extent and effectiveness of fracture–matrix interactions in unsaturated rocks. The data obtained in some of the larger field experiments have been used to develop or test a range of flow and transport models for Yucca Mountain. A few modeling studies are cited in this section because their authors also provide details about the experiments. However, a detailed analysis and evaluation of the modeling studies is not provided in this report, which focuses instead on the experiments and the data that the tracer tests have provided for the modeling studies.

2.1 Alcove 8–Niche 3 Experiments

The Alcove 8–Niche 3 experiments were large-scale tests located in two of the same lithostratigraphic zones of the Topopah Spring Tuff as the potential repository (Table 2-1). Broadly, the tests were designed to evaluate unsaturated zone flow, seepage response, and matrix diffusion processes in densely welded tuff. A specified goal was to provide quantitative support for fracture system hydrologic properties and the active fracture model (Liu, et al., 1998). Descriptions of the Alcove 8–Niche 3 tests are provided in recent papers by Salve (2005), Salve, et al. (2004), and Zhou, et al. (2006), and in several DOE documents, including Analysis of Alcove 8 and Niche 3 Flow and Transport Tests (Bechtel SAIC Company, LLC, 2006), *In-Situ* Field Testing of Processes (Bechtel SAIC Company, LLC, 2004a, Section 6.12), Technical Basis Document No. 10: Unsaturated Zone Transport (Bechtel SAIC Company, 2004b, Section 4.2.2), and Technical Basis Document No. 3: Water Seeping into Drifts (Bechtel SAIC Company, LLC, 2004c, Appendix H).

Alcove 8 was excavated from the Enhanced Characterization of the Repository Block Cross-Drift where the cross drift passes above the main drift of the Exploratory Studies Facility (Figure 2-1). Niche 3, also referred to as Niche 3107, is a small extension off the Exploratory Studies Facility main drift. To maintain high relative humidity and to reduce ventilation-induced drying, bulkheads at the room entrances isolated Alcove 8 and Niche 3 from direct ventilation in the main access tunnels during the experiments. Niche 3 is directly beneath Alcove 8, separated by about 21 m [70 ft] of densely welded tuff. Alcove 8 is located in the Topopah Spring upper lithophysal (Tptpul) zone of the Topopah Spring welded tuff. The lithophysae are naturally occurring cavities up to 0.75 m [2.5 ft] wide and up to 0.3 m [1 ft] high. The majority of fractures in the Tptpul zone are small features around the lithophysae and are thought to be cooling features (Bechtel SAIC Company, LLC, 2004a). Niche 3 is located in the middle nonlithophysal (Tptpmn) zone, which is a densely welded, highly fractured devitrified tuff containing no lithophysal cavities. The lithological contact between the two zones is approximately midway between Alcove 8 and Niche 3. A distinctive feature of Alcove 8 is a minor near-vertical fault that cuts through the alcove. The fault is open on the alcove ceiling, appears to be closed on the floor, and is visible as a fracture in the ceiling of Niche 3.

Table 2-1. Yucca Mountain Unsaturated Zone Stratigraphy and U.S. Department of Energy Field Test Horizons

Excavation Name and Location*	Lithostratigraphic Nomenclature and Abbreviations†		Hydrogeologic Units‡
	Alluvial and colluvial deposits (Quaternary)	QTac	not included
	TIMBER MOUNTAIN GROUP (Tm)		
	Rainier Mesa Tuff	Tmr	
	PAINTBRUSH GROUP (Tp)		
	Tiva Canyon Tuff (Tpc)		
	Crystal-rich member	Tpcr	
	Crystal-poor member	Tpcp	
ESF Alcove 1 →	Upper lithophysal zone	Tpcpul	
	Middle nonlithophysal zone	Tpcpmn	Tiva Canyon Welded Unit (TCw)
	Lower lithophysal zone	Tpcpll	
	Lower nonlithophysal zone	Tpcpln	
	Vitric zone	Tpcpv	
	Densely welded	Tpcpv3	
	Moderately welded	Tpcpv2	
	Nonwelded	Tpcpv1	Paintbrush Nonwelded Unit (PTn)
	Pre-Yucca Mountain Tuff bedded tuff	Tpbt3	
ESF Alcove 4 →	**Pah Canyon Tuff (Tpp)**		
	Pre-Pah Canyon Tuff bedded tuff	Tpbt2	
	Topopah Spring Tuff (Tpt)		
	Crystal-rich member	Tptr	
	Vitric zone	Tptrv	
	Nonwelded	Tptrv3	
	Moderately welded	Tptrv2	
	Densely welded	Tptrv1	Topopah Spring Welded Unit (Tsw)
	Nonlithophysal zone	Tptrn	
	Lithophysal zone	Tptrl	
	Crystal-poor member	Tptp	
ECRB Alcove 8 →	Upper lithophysal zone	Tptpul	
ESF Alcove 6, Niches 2, 3 , 4 →	Middle nonlithophysal zone	Tptpmn	
	Lower lithophysal zone	Tptpll	
	Lower nonlithophysal zone	Tptpln	
	Vitric zone	Tptpv	
Busted Butte Test Facility →	Densely welded	Tptpv3	
	Moderately welded	Tptpv2	
Busted Butte Test Facility →	Nonwelded	Tptpv1	Calico Hills Nonwelded Unit (CHn)
	(Pre-Topopah Spring Tuff bedded tuff)	Tpbt1	
	CALICO HILLS FORMATION	Tac	
Busted Butte Test Facility →	Bedded tuff	Tacbt	
	Basal sandstone	Tacbs	
	CRATER FLAT GROUP		
	Prow Pass Tuff (Tcp)		
	Pre-Prow Pass bedded tuff	Tcpbt	
	Bullfrog Tuff (Tcb)		
	Upper vitric nonwelded	Tcbuv	
	(all other Bullfrog Tuff zones)		Crater Flat undifferentiated Unit (CFu)
	Tram Tuff (Tct)		
	(all zones)	Tct	

* Test horizons indicated by arrows. Shaded stratigraphic zones are intersected by potential repository horizon.
ESF, Exploratory Studies Facility; ECRB, Enhanced Characterization of the Repository Block.
† Nomenclature and units from Bechtel SAIC Company, LLC. "Analysis of Geochemical Data for the Unsaturated Zone." ANL–NBS–HS–00017. Rev 00 ICN 02. Las Vegas, Nevada: Bechtel SAIC Company, LLC. 2002.
‡ Unit boundaries from Bechtel SAIC Company, LLC. "Yucca Mountain Site Description." TDR–CRW–GS–000001. Rev 02 ICN 01. Las Vegas, Nevada: Bechtel SAIC Company, LLC. 2004.

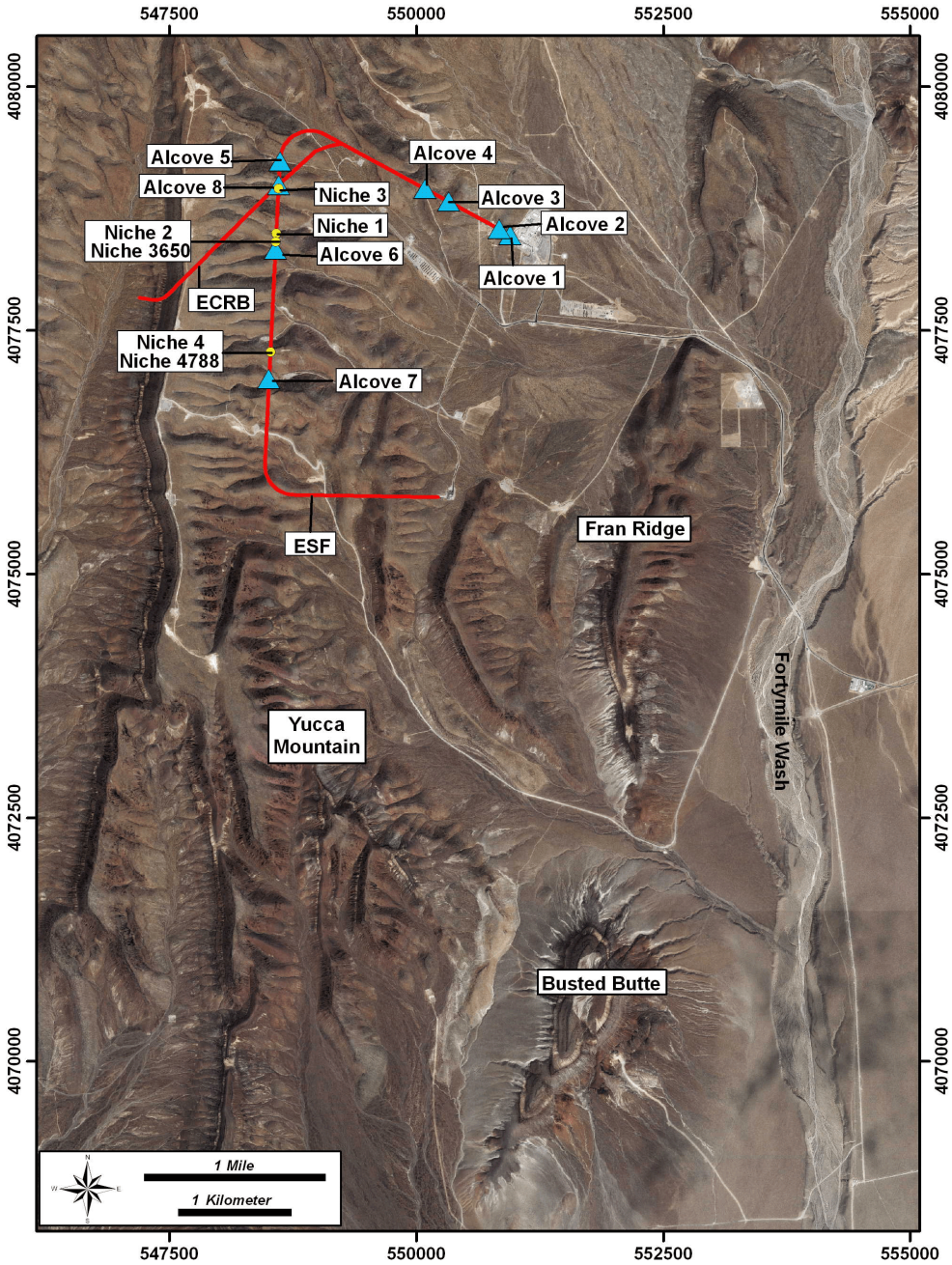

Figure 2-1. Underground Alcoves and Niche Locations in the Exploratory Studies Facility and Extended Characterization of the Repository Block Tunnel in the Yucca Mountain—Busted Butte Area of Southern Nevada

2.1.1 Fault Infiltration Test

Two major *in-situ* infiltration and seepage tests, informally known as the fault test and the large-plot test, were conducted in the Alcove 8–Niche 3 program. The fault test, completed in 2002, included tracer studies that DOE interpreted in the context of matrix diffusion processes (e.g., Salve, et al., 2004). In the fault infiltration test, water was introduced into a shallow, narrow trench that had been excavated in the floor of Alcove 8 along the trace of the fault {about 5 m [16.4 ft]}. Beginning in early March 2001, ponded water was released for more than a year along the full length of the fault trace. The migration of the wetting front through the rock was monitored in several slanted boreholes fitted with electrical resistivity probes to measure changes in saturation of the adjacent rock. Seepage into Niche 3 was first observed in the ceiling in early April 2001, about 5 weeks after the experiment began. In October 2001 after quasi-steady state seepage conditions were attained, two nonsorbing tracers with different molecular diffusion coefficients (bromide and pentafluorobenzoic acid) and a sorbing tracer (lithium) were released into the fault for 9 days, followed by tracer-free water for the next 6 months. Tracer concentrations were sampled and monitored in three of the trays that collected seepage waters from the ceiling of Niche 3.

In the tray that had the lowest seepage flux, low concentrations of bromide and pentafluorobenzoic acid were first detected 3 weeks after the initial release of tracers into the fault. The concentration of both tracers gradually increased over several weeks, although the seepage concentration of bromide relative to its starting concentration remained lower than the relative concentration of pentafluorobenzoic acid. Given the nonsorbing behavior of these tracers, the low relative concentration of both tracers was attributed to diversion of some of the tracer into the rock matrix, slowing its overall transport rate. The likelihood that matrix diffusion contributed to this effect was suggested because the observed rise in pentafluorobenzoic acid concentration preceded the observed rise in bromide concentration, which is consistent, in terms of diffusion coefficients, with the relative molecule sizes of the two species.

In the trays that had the highest seepage flux, the rise in pentafluorobenzoic acid concentration again preceded the rise in bromide concentration, but the magnitudes and arrival times of the two tracers were similar to each other. DOE attributed these effects to the involvement of different fracture pathways such that more rapid flow reduced the effectiveness of matrix diffusion. In the DOE analysis of results, this conclusion was also supported by the behavior of lithium, the sorbing tracer. Its transport was retarded significantly by sorption compared to the nonsorbing tracers, but it still arrived sooner and in slightly higher concentration in the tray with the highest seepage flux than in the tray with the lowest seepage flux. Fewer opportunities for matrix diffusion or for sorption would be expected along a more direct or rapid transport pathway.

At the conclusion of the fault tracer observations in April 2002, the water supply system was switched from saturated application (ponded) to unsaturated application by supplying a known amount of water per minute to the fracture using pumps, while continuing to monitor the moisture patterns in the rock and seepage into Niche 3. The water supply rate was further reduced in July 2002, and the test was stopped in August 2002. A planned second phase of the fault test to examine the transport of tracers at lower infiltration rates was canceled.

2.1.2 Large-Plot Infiltration Test

The other major field test in Alcove 8–Niche 3 was the large-plot infiltration test, in which ponded water was released simultaneously from twelve 1-m [3.3-ft] squares in a 3 × 4-m [9.8 × 13.1-ft] grid on the floor of Alcove 8 (Salve, 2005; Zhou, et al., 2006). The grid covered a number of previously mapped fractures on the alcove floor. One corner of the large-plot infiltration grid was near, but did not intersect, the exposed fault trace of the earlier test. Moisture content changes in the rock were monitored with sets of regularly spaced electrical resistivity probes in two horizontal 9-m [29.5-ft] boreholes located parallel to and 1 m [3.3 ft] above the axis of the ceiling of Niche 3 and in seven 6-m [19.7-ft] boreholes that extended from the side and rear walls of the niche in a radiating pattern. The monitoring boreholes around Niche 3 were separated from the infiltration plot in the floor of Alcove 8 by a vertical distance of about 20 m [65.6 ft].

The first phase of the large-plot test commenced as an infiltration and seepage experiment (no special tracers) in August 2002 and ended in March 2003. A total of about 23,000 L [6,076 gal] of water infiltrated the rock during this period. At the beginning of the experiment, the ponded infiltration rate increased rapidly over the first 4 weeks to about 350 L/d [92.5 gal/d], then it decreased over the next 6 weeks to about 75 L/d [19.8 gal/d]. Over the next 8 weeks, the rate at which water was entering the rock decreased gradually to about 40 L/d [10.6 gal/d], and the rate remained at or near this value for the rest of the experiment. The gradual decrease in infiltration rate to a steady-state value conformed with results in other fractured rock experiments at Yucca Mountain that have been attributed to a heterogeneous fracture network in which open, poorly connected fractures tend to fill with water early and remain saturated throughout the remainder of the test (Salve, et al., 2002).

Thirteen days after the large-plot infiltration experiment began, the first arrival of water was detected in one of the horizontal monitoring boreholes directly above the ceiling of Niche 3. Over the next 60 days, wetting fronts were detected by electrical resistivity probes in all nine of the monitoring boreholes. Some wetting of the back wall near the ceiling in Niche 3 was observed 3 weeks after the infiltration test commenced, and measurable seepage was noted there about 1 week later. From the location and arrival time of the flow's leading edges, at least seven large flow paths {arbitrarily classified as being wider than about 1 m [3.3 ft]} and a few distinct smaller flow paths were identified. Complete wetting occurred rapidly along the fast flow paths but more slowly in other locations. The fastest observed velocities {about 1.7 m/d [5.6 ft/d]} were in a flow pathway about 0.5-m [1.6-ft] wide that shifted by a lateral distance of about 4.75 m [15.6 ft] relative to the 22 m [72.2 ft] vertical distance between the infiltration plot and the boreholes. Sections of this flow path diverged and were separated by up to 1 m [3.3 ft] of rock that remained unwetted throughout the test.

The large-plot grid arrangement allowed infiltration rates to be measured for each square in the grid. There was a positive correlation between the infiltration rate and the fracture density in each square, but there was no similar correlation between the fracture density on the ceiling of Niche 3 and the rate and location of the seepage.

The last stages of the large-plot infiltration test, including tracer tests, are documented in Analysis of Alcove 8/Niche 3 Flow and Transport Tests (Bechtel SAIC Company, LLC, 2006). In Stage 2, the supply of water to 10 subplots was interrupted from March 2003 until August 2003, and water was supplied (ponded conditions) to only 2 subplots. The infiltration rates in these

two subplots (which had the highest near-constant infiltration rates during Stage 1) did not appear to be significantly affected by the removal of water from the neighboring subplots. However, the Stage 2 seepage rates dropped to nearly zero throughout Niche 3.

Stage 3 commenced in August 2003 when infiltration was resumed (ponded conditions) in all 12 subplots in Alcove 8. After a lag of about 30 days, comparable to the timing of first seepage in Stage 1, the Stage 3 daily seepage rates in Niche 3 quickly climbed to 10–15 L [2.6–4.0 gal] per day, fluctuated over the next 5 months, then gradually began declining, although the total infiltration rate during most of Stage 3 remained similar to the rate that had been observed at the end of Stage 1. The tracer tests commenced in March 2004, when pairs of nonreactive tracers were added to the infiltration water for several weeks. The infiltration subplots were divided into three zones for the tracer tests, and each zone received two distinct tracers (2,6-Difluorobenzoic Acid and potassium iodide; 2,5-Difluorobenzoic acid and calcium bromide; or 2,4,5-Trifluorobenzoic acid and potassium fluoride). However, Niche 3 seepage rates continued to decline to very low levels after the tracer tests began, and no tracers were observed in any of the seepage samples. In August and September of 2004, water was removed briefly from several infiltration subplots in Alcove 8, and biofilms and fine debris were scrubbed from the floors. In subplots 1 and 2, there was an immediate increase in infiltration rates after scrubbing, accompanied by a rapid increase in seepage rates in Niche 3. Low but reliable tracer arrival signals were observed in this seepage for iodine and 2,6-Difluorobenzoic acid, which were the tracers injected in subplots 1 and 2. Although other tracers in some of the seepage samples also appeared to have a small increase above background levels, the concentrations were so low that the investigators did not consider these data to be reliable breakthrough indicators.

Infiltration was stopped in the large-plot test in October 2004, approximately 800 days after the test began, and seepage was monitored for several more weeks. A planned Phase II of the large-plot infiltration test with lower (nonponded) infiltration conditions was not implemented.

In comparing predicted and observed infiltration and transport behavior in the large-plot test, the investigators noted that the test demonstrated the complexity of flow processes at the test site and how this complexity hindered the interpretation of test results by modeling. The investigators proposed that downward-moving debris particles (from excavation of Alcove 8) may have caused the observed fluctuations in infiltration rates and sharp decreases in seepage rates. If that were the case, the infiltration pulse late in Stage 3 that occurred after scrubbing the infiltration subplots may have dislodged particles from fractures near Niche 3, allowing water and tracers to access the seepage flow paths again. The investigators pointed out that these arguments are supported by results from a laboratory and field study of particle transport in unsaturated fractured limestone (Weisbrod, et al., 2002). Similarly, other recent studies have considered the effect of biofilm formation on transmissivity experiments in fractured limestone (e.g., Arnon, et al., 2005).

Another unanticipated result of the large-plot infiltration test was that essentially none of the applied tracers were recovered in the Niche 3 seepage over the observation period of more than 6 months, though considerable concentrations of tracers were predicted for this time period. The investigators proposed that matrix diffusion had been more effective than expected over the test interval, leading to low relative concentrations of tracers in the recovered seepage. The low tracer recoveries were simulated in posttest analyses by greatly increasing the size of the effective matrix diffusion coefficient. The investigators noted that tracer studies in field

experiments elsewhere have suggested that (i) the effective matrix diffusion coefficient is scale dependent or (ii) the effective fracture–matrix interface area is larger because there are more conductive fractures in a natural setting than are represented in a simplified model.

Salve (2005) noted that the large-plot infiltration test conformed with other studies indicating the importance of preferential flow pathways in fractured rocks, but that, more importantly, insights from the large-plot test have the potential to improve existing conceptual models of how water moves through unsaturated fractured rock. Water movement patterns in the large-plot infiltration tests were dictated by a network of numerous fractures of various sizes that defined a heterogeneous set of flow conduits. Salve (2005) concluded that although capillary diversion may have accounted for some water movement around Niche 3, most of the lateral flow appears to have resulted from the geometry of the fracture network itself. Although Niche 3 was located 20 m [65.6 ft] directly beneath the infiltration plot in Alcove 8, only 10 percent of the total volume of water released from Alcove 8 was collected as seepage in Niche 3.

In an evaluation of the role of fracture data in modeling unsaturated flow and transport processes at Yucca Mountain, Hinds, et al. (2003) concluded that the subset of large-scale fracture data DOE used was appropriate for mountain-scale flow models but that smaller fractures may be of particular importance for transport processes. Similarly, on the basis of observations from the Alcove 8/Niche 3 infiltration tests, Salve (2005) suggested that conceptual models for unsaturated zone transport should be defined at a finer scale than for flow models, given that small, interconnected fractures {less than 1 m [3.28 ft] in length} may enhance matrix diffusion and contribute to the storage capacity of the rock.

2.2 Liquid Release and Tracer Studies in Unsaturated Fractured Welded Tuffs (Alcove 6)

Salve, et al. (2002) and Hu, et al. (2001) reported field experiments involving localized releases of tracer-laced water in the middle nonlithophysal zone (Tptpmn) of the Topopah Spring welded tuff (Table 2-1). The experiments, conducted in Alcove 6 of the Exploratory Studies Facility at Yucca Mountain (Figure 2-1), used small amounts of water released periodically from a fixed injection location as an analog for localized movement of contaminated fluid in a repository setting, either as a result of an individual waste package failure or due to transient high-infiltration events. The objective of the Alcove 6 liquid release study (Salve, et al., 2002) was to estimate hydraulic parameters such as formation intake rates (the rates at which ponded water flows into fractured rock), flow velocities (inferred from the time taken for a wetting front to travel a known distance), and percolation rates through the zone of interest. The objective of the Alcove 6 tracer study (Hu, et al., 2001) was to use different sets of multiple tracers to investigate flow and transport in the fractured tuff in response to various liquid release rates.

The liquid release and tracer studies examined fracture flow and fracture–matrix interaction on a scale of several meters. At this location in the Exploratory Studies Facility, the tuff was visibly fractured, with predominantly vertical fractures spaced tens of centimeters apart and few subhorizontal fractures. A horizontal seepage collection slot, 2 m [6.6 ft] wide by 0.3 m [1 ft] high by 4 m [13.1 ft] deep, was excavated in Alcove 6 near the bottom of a side wall. The slot was fitted with a set of 28 retrievable stainless steel compartments to collect any seepage from above during the tests. Four boreholes were drilled horizontally, each to a distance of 4 m [13.1 ft] into the wall above the slot. One borehole, located about 1.6 m [5.2 ft] above the

centerline of the slot, was used as the injection borehole. It was fitted with an inflation packer system that isolated two injection zones: a low-permeability zone and a high-permeability zone. The other three boreholes, one located beside the injection borehole and the other two below it, were fitted with electrical resistivity probes and psychrometers to monitor changes in water saturation and ionic strength. Water that seeped into the trays in the excavated slot underneath the boreholes was transferred to water collection bottles, where it was measured and analyzed for tracers.

2.2.1 Alcove 6 Liquid Release Tests

The liquid release study (Salve, et al., 2002) was divided into a low-permeability zone experiment and a high-permeability zone experiment in which the differences in permeability were attributed largely to different fracture sets. Permeabilities of the injection zones were determined from air-permeability measurements conducted over 0.3-m [1-ft] sections along the borehole, which identified the least permeable zone at a distance of 0.75 to 1.05 m [2.5 to 3.4 ft] from the borehole collar and the most permeable zone at 2.3 to 2.6 m [7.5 to 8.5 ft] from the borehole collar. The zones were isolated in the borehole by inflatable rubber packers during the liquid release tests. The experiments were conducted over two consecutive 3-week intervals beginning in July 1998. In the low-permeability zone experiment, tracer-laced water was released from the injection borehole into the low-permeability zone in three separate tests, followed by monitoring of the wetting front for each test. In the high-permeability zone experiment, water was injected into the high-permeability zone during eight separate tests, which were divided into two groups. The first high-permeability group of tests used tracer-laced water. The second high-permeability group of tests was tracer-free except for lithium bromide. (A lithium bromide spike is added to all water used in the Exploratory Studies Facility mining activities and most experimental activities.)

In the first low-permeability zone test, the liquid-intake rate initially was relatively high {about 16 mL/min [0.5 oz/min]} due to imbibition in the unsaturated rock matrix, but infiltration gradually decreased to a steady state of about 0.35 mL/min [0.01 oz/min]. The liquid-intake rate in the next two low-permeability zone tests remained low, even after pauses of several days between tests. The monitoring borehole that was directly beside and parallel to the injection borehole never detected any wetting of the rock, even though the two boreholes were only 1 m [3.28 ft] apart. Changes were detected, however, in the other two monitoring boreholes, which were located 0.7 m [2.3 ft] below the injection borehole and 0.7 m [2.3 ft] apart from each other. The most extreme change in saturation along the length of the boreholes was detected nearest to the alcove wall, where the rock had been previously exposed to drying effects from ventilation in the main drift of the Exploratory Studies Facility. At distances of about 2 m [6.6 ft] and more from the wall, the changes in saturation in the boreholes were much smaller. No seepage from the slot ceiling occurred during any of the release tests in the low-permeability zone.

In the first group of tests in the high-permeability zone experiment (Tests 1, 2, 3, and 4), the water releases in Tests 1 and 2 were conducted under constant-head conditions to determine the maximum rate at which the zone would take in water. The intake rates fluctuated considerably during and between these tests. In Test 1, which lasted for slightly more than 2 hours, the liquid-intake rate increased during the first hour from about 80 mL/min [2.7 oz/min] to about 130 mL/min [4.4 oz/min], after which it spiked sharply to an intake rate of about 180 mL/min [6.1 oz/min] and then fluctuated repeatedly between 70 and 160 mL/min [2.4 and 5.4 oz/min] for the remainder of the test. In Test 2, which lasted about 3 hours, the intake rate

briefly increased from 80 to 130 mL/min [2.7 to 4.4 oz/min] initially, then leveled off at about 100 mL/min [3.4 oz/min]. After 90 minutes, the intake rate decreased sharply to 35 mL/min [1.2 oz/min], then increased to 130 mL/min [4.4 oz], and finally leveled off to about 90 mL/min [3.0 oz/min] for the remainder of the test. The average intake rate was 119 mL/min [4.0 oz/min] for Test 1 and 98 mL/min [3.3 oz/min] for Test 2. On the basis of the first two tests, water in Tests 3 and 4 was supplied at fixed rates of 53 mL/min and 5 mL/min [1.8 oz/min and 0.2 oz/min]. The second group of tests used moderately high but successively lower fixed release rates of 69, 38, 29, and 14 mL/min [2.3, 1.3, 1.0, and 0.5 oz/min] for Tests 5, 6, 7, and 8.

In contrast to low-permeability zone tests, seepage was observed from all eight tests in the high-permeability zone. In Tests 1, 2, and 3, water appeared at the slot ceiling within 5 minutes. At the much lower release rate of Test 4, water appeared after 5 hours. In the second group of high-permeability zone tests, water appeared within 7 minutes in all but Test 8, where it appeared within 68 minutes. The seepage in all tests was intermittent rather than steady. Except in Tests 4 and 8, in which release rates were very low, each test recovered between 60 and 80 percent of the injected water.

Although the low-permeability zone and the high-permeability zone were only 1 m [3.28 ft] apart in the injection borehole, the formation response to the releases of liquid in each zone demonstrated significant variability. Salve, et al. (2002) noted that the behavior of the low-permeability zone suggested a conceptual flow model consisting of a strongly heterogeneous fracture network in which the high-permeability fractures are not extensive or are poorly connected and dead-end fractures wet up early and remain saturated, so that smaller interconnected fractures controlled the long-term water uptake rate. In contrast, the intake rates in the high-permeability zone did not show consistent decreases as more water entered the system, but instead the rates fluctuated significantly, as did the seepage rates. Salve, et al. (2002) observed that these behaviors suggested a conceptual model dominated by high-conductivity, well-connected flow paths in which flow occurred in a few preferential, channelized pathways within the fractures.

2.2.2 Alcove 6 Tracer Results

Tracers were used in the low-permeability zone tests, but no tracers were recovered because no seepage water was recovered for any tests in the low-permeability zone. In the high-permeability zone experiments, a different fluorobenzoic acid was used as a tracer in each of Tests 1, 2, 3, and 4. In Tests 1 and 2, no matrix interactions were observed. Full concentrations (in which the recovered concentration was equal to the starting concentration, $C = C_0$) of the tracers were recovered in the seepage trays that were correlated with the fastest travel paths. Some of the other trays did not collect any seepage during the first test, but tracers from Test 1 were detected in seepage to one of these trays during Test 2. According to Hu, et al. (2001), this indicated that some secondary flow pathways that were not obvious in Test 1 continued to be active in Test 2.

At the lower release rates of Tests 3 and 4, the relative concentration of the recovered tracers was lower, indicating that some of the tracer in each test was being slowed. This effect was most pronounced for Test 4, which had the lowest release rate in this group, the smallest amount of seepage, and at a steady-state value of $C/C_0 = 0.55$, the lowest concentration of

tracer relative to the starting concentration. Hu, et al. (2001) noted that the much longer travel time for the tracer, which was not in proportion to the infiltration rate, suggested that a significant proportion of the tracer had moved from the fracture network into the matrix.

The remaining four tests in the high-permeability zone did not contain any fluorobenzoic acid tracers, but the seepage water was analyzed in each test. Seepage in Test 8, which had a low infiltration rate comparable to Test 4, contained some of the tracer from Test 4. Hu, et al. (2001) concluded that the water at low infiltration rates followed similar flow paths.

2.3 Infiltration Tests in Tiva Canyon Welded Tuff (Alcove 1)

In 1998–1999, DOE conducted near-surface infiltration tests at Yucca Mountain in Alcove 1 of the Exploratory Studies Facility (Figure 2-1). The alcove, located near the north portal of the facility, was excavated underneath a 7.9 by 10.6 m [26 by 35 ft] infiltration plot at the ground surface. The infiltration plot and the alcove were separated by about 30 m [98 ft] of fractured, densely welded rock from the upper lithophysal zone of the Tiva Canyon tuff (Table 2-1). Water was supplied to the tests from irrigation drip tubing in which 490 drippers were uniformly distributed across the plot (Liu, et al., 2003). The drip rates were varied during the tests, but all of the applied rates were less than the estimated fracture-saturated hydraulic conductivity. The infiltration plot was covered with a plastic sheet to reduce evaporative water loss. To simulate the transient nature of infiltration in the unsaturated zone at Yucca Mountain, applied infiltration rates in Phase I tests varied from rates near zero to about 5 cm/d [0 to 2.0 in/d]. Phase II tests, which commenced about 4 months after the Phase I tests ended, generally involved lower and less variable infiltration rates between 1 and 3 cm/d [0.4 and 1.2 in/d]. During the late stage of Phase II, bromide, a nonreactive tracer, was added to the water supply, and a fairly constant applied infiltration rate of about 2.5 cm/d [1.0 in/d] was maintained for about 90 days.

Total seepage from the infiltration plot into Alcove 1 was collected using 432 collection trays placed just below the ceiling of the alcove to provide coverage of the entire ceiling. During the tests, a bulkhead isolated the alcove from the main tunnel to maintain high relative humidity in the alcove and reduce ventilation-related evaporation from the alcove walls. Seepage rates were approximated by dividing the amount of water collected in the trays by the interval of time, usually about 1 day, in which the water had accumulated. By analyzing the seepage water, tracer concentrations were obtained during the same collection interval. The bromide concentration in the recovered seepage was low relative to the starting concentration—an effect which was attributed to matrix diffusion (Liu, et al., 2003).

2.4 Penetration of Dyes From Fractures Into Welded Tuff Matrix (Niche 2 and Niche 4)

The imbibition of water by capillary forces from a flowing fracture into unsaturated rock matrix pores is another unsaturated zone process that potentially slows contaminant transport. Hu, et al. (2002) conducted field and laboratory experiments to investigate the extent that dyes and other tracers penetrated unsaturated, fractured rock matrix by imbibition. The field tests were primarily conducted to observe flow pathways qualitatively, after which samples of rock from the flow path were tested in the laboratory to study the extent of tracer penetration in more detail.

Field tests were conducted in the Exploratory Studies Facility in the densely welded middle nonlithophysal zone of the Topopah Spring tuff (Table 2-1). Prior to excavating Niche 2 (also referred to as Niche 3650) and Niche 4 (also referred to as Niche 4788) in the Exploratory Studies Facility, horizontal boreholes were dry-core drilled into the drift wall at the planned niche locations, and water containing fluorescent tracers or food dyes (rhodamine or FD&C Blue No.1) was pumped for short periods (8–35 minutes) at a constant rate into 0.3-m [1-ft]-long test intervals isolated by a straddle packer system in the boreholes. The test intervals were located more than 6 m [19.7 ft] into the rock to minimize the effects of previous drying of the rock matrix due to ventilation in the main drift. Within 1–2 weeks after the dye-laced water {about 1 L [1 qt] per interval} had been released into the rock, the boreholes were mined out during excavation of the niches. Distribution of the dyes was observed and recorded during the mineback operations, and samples of the dye-stained rocks were collected for additional laboratory analysis.

The dye left distinct stains on the fracture surfaces but was not visible in the matrix within a few millimeters from the fracture surface. In chemical profiles of samples, the dye could not be detected more than 6 or 7 mm [0.2 or 0.3 in] from the fracture surface in all cases. According to Hu, et al. (2002), these results demonstrated that imbibition occurred discernibly over a short time under *in-situ* conditions in partially saturated, densely welded tuff. A calculated imbibition penetration depth, based on measured rock properties of Topopah Spring tuff, was in good agreement with the measured penetration depth.

In the laboratory tests, cores were cut from a tracer-free block of tuff from Station 44+00, from the same middle nonlithophysal zone of tuff as in Alcoves 2 and 4. The cores were equilibrated in relative humidity chambers to obtain initial partial saturations of 12 and 76 percent. To simulate imbibition and penetration by capillarity, the cores were suspended for 16–18 hours inside a humidity-controlled chamber with the bottom of the core submerged about 1 mm [0.39 in] in a solution containing one of two mixtures of dyes and nonsorbing tracers with different molecular sizes. At high initial water saturation (83 percent), most of the pores in the matrix were filled with water. The movement of the tracers through the matrix lagged considerably behind the progression of the wetting front. The concentration profiles for bromide and the two tracers with larger molecular sizes (pentafluorobenzoic acid and hydroxypropyl-β-cyclodextrin) were identical, even though there were large differences in their diffusion coefficients, which Hu, et al. (2002) concluded was an indication that mechanical dispersion, not diffusion, was responsible for the delayed migration of the tracers through the matrix. In contrast, at low initial water saturation (15.2 percent), more of the matrix pore spaces initially were dry, and all of the tracers traveled farther into the matrix by imbibition than they did at high saturation. Hu, et al. (2002) reported that the transport of bromide, which could enter a wider range of pore sizes during imbibition than the larger tracer molecules, coincided with the wetting front itself. Overall, Hu, et al. (2002) concluded that the tests provided visual evidence of fracture flow pathways and demonstrated that significant matrix imbibition can occur during a flow event, even on a timescale of a few hours, in partially saturated, low permeability welded tuff.

2.5 Fault–Matrix Interactions in Nonwelded Tuff of the Paintbrush Group (Alcove 4)

Nonwelded air-fall tuffs of the Paintbrush Group directly overlie the densely welded Topopah Spring tuffs (Table 2-1). To investigate fast flow potential through the nonwelded, pumice-rich tuffs at Yucca Mountain, Salve, et al. (2003) carried out *in-situ* infiltration experiments at Alcove 4 in the Exploratory Studies Facility (Figure 2-1). The experiments released water either along a minor subvertical fault or directly into the porous matrix of the Paintbrush Group nonwelded tuffs. The experiment design was similar to the Alcove 6 tests (Section 3.2), where test water was released from boreholes drilled horizontally into the alcove wall. The progression of the wetting front through the rock was monitored by a set of boreholes and a wide seepage collection slot excavated into the lower part of the alcove wall underneath all the boreholes. After the experiment setup was in place, various sets of release experiments were conducted in Alcove 4 over a period of about 16 months from October 1998 to February 2000. The repeated releases allowed differences to be observed in flow and imbibition behavior due to the migration of a wetting front and changes in matrix saturation.

The test area was located at the far end of Alcove 4, in the back wall of the room. Alcove 4 is about 210 m [689 ft] below ground surface and transects portions of the lower Pah Canyon Tuff and the upper Pre-Pah Canyon bedded tuffs (Table 2-1). A small, clearly visible normal fault with an offset of about 0.25 m [0.8 ft] cuts the back wall of the alcove and extends into rock behind it. A set of horizontal boreholes, each 6 m [19.7 ft] long, was drilled perpendicular to the alcove face in the vicinity of the fault. Three of the boreholes were positioned to intersect the fault plane where it extended into the rock beyond the alcove face. Another set of horizontal 6-m [19.7-ft]-long boreholes was drilled in the upper right portion of the alcove face, away from the fault plane, to investigate water flow through the nonwelded tuffs in the absence of a fast flow path. The uppermost borehole in both sets was used as the water supply system for the infiltration experiments. The remaining boreholes were fitted with electrical resistance probes and psychrometers to monitor changes in saturation and ionic strength. Near the floor of the alcove, a horizontal slot 6 m [19.7 ft] wide, 0.3 m [1 ft] high, and 4 m [13.1 ft] deep was excavated underneath the entire array of boreholes. The slot was fitted with a water collection system to monitor any seepage that might occur during the experiments.

In October 1998, water was released from two intervals along the borehole in the tuff matrix. Approximately 1 year later, water again was released from one of the intervals. In each test, the intake rate initially was high but dropped sharply after a few hours and asymptotically approached low steady-state values of about 0.1 mL/min [0.03 oz/min]. The migration of the wetting fronts, as monitored by boreholes, indicated that there were several small, discrete pathways in the matrix that allowed water to move relatively rapidly over distances of about a meter, although the matrix as a whole was not capable of transmitting water at this rate. Except for a damp spot that developed in the slot ceiling near the end of the experiments, no seepage was observed.

In the injection borehole that intersected the fault, water was released in a series of 10 tests. In the first seven release tests, conducted sequentially in October and November 1998, the intake rate declined during each test, and the overall intake rate in each test was smaller than that of the preceding test. Following the seventh test, no water was released into the fault for approximately 1 year. During this time, the fault itself showed a decrease in saturation almost

immediately, and the nearby matrix (as detected in the monitoring boreholes) exhibited a slow drying trend over many months. In November and December 1999, the remaining three release tests were conducted. The intake rates for these tests mimicked the first three release tests, suggesting that the tuff matrix had returned to its original saturation condition.

Based on the observed intake rates, flow-path volumes, and progression of wetting fronts along the fault, Salve, et al. (2003) concluded that the movement of water along this flow path was influenced by the wetting history. Salve, et al. (2003) suggested that water from an episodic infiltration event entering a potentially fast flow path such as a fault in the Paintbrush Tuff would move along the path in two stages. First, the wetting front around the fault would move slowly outward as water was absorbed by the matrix. Second, as the matrix became wetter, more of the water would travel down the fault. Equal volumes of water released in quick succession along such a wetted pathway could potentially travel farther than through the matrix alone. This effect would be lessened, however, by the significant reduction in the rate at which water is able to enter the fast flow path, as was indicated by the progressively declining intake rates in the first seven tests.

2.6 Transport Tests in Calico Hills Nonwelded Tuff (Busted Butte Test Facility)

The Calico Hills Formation is the main stratigraphic unit below the potential repository at Yucca Mountain in which unsaturated-zone transport by matrix flow is expected to be more significant than fracture flow. Accordingly, the Busted Butte tests were a set of long-term experiments to investigate flow and transport in the nonwelded tuffs. Descriptions of the Busted Butte field tests are provided in several DOE documents, including *In-Situ* Field Testing of Processes (Bechtel SAIC Company, LLC, 2004a, Section 6.13), Unsaturated Zone and Saturated Zone Transport Properties (Bechtel SAIC Company, LLC, 2001) and Technical Basis Document No. 10: Unsaturated Zone Transport (Bechtel SAIC Company, LLC, 2004b).

The Busted Butte transport tests, which demonstrated a high degree of interconnected porosity in the matrix, indicated the prevalence of matrix flow in the rocks in which the tests were conducted. Fracture flow was not a dominant mechanism, but the experiments examined fracture–matrix interactions where a permeability contrast was noted. Attempts were made to obtain data about the transport of contaminants through the matrix by pairing conservative (nonreactive) tracers that had different diffusion coefficients and looking for differences in their breakthrough curves.

Busted Butte is located approximately 8 km [5 mi] southeast of Yucca Mountain (Figure 2-1). The underground test facility exposes the lithostratigraphic contact between the Topopah Spring Tuff and the Calico Hills Formation (Table 2-1). At this location, the lowermost unit of the Topopah Spring Tuff is a vitrophyre that is densely welded and fractured at the top (Tptpv3), grades downward into a less welded and less fractured zone (Tptpv2), and then grades into a nonwelded and permeable base (Tptpv1), in contact with the nonwelded tuffs of the Calico Hills Formation (Table 2-1). The Busted Butte transport tests involved the Topopah Spring units Tptpv2 and Tptpv1 and the upper portion of the Calico Hills Formation.

The tracer tests, conducted from April 1998 to October 2000, were conducted by drilling sets of injection boreholes and collection boreholes horizontally into an excavated wall of the facility,

followed by mineback or overcoring at the end of the test stage to obtain more detailed information about faults and permeability contrasts and to examine rock samples for tracer dyes indicating flow paths. Unlike many of the experiments in the Exploratory Studies Facility, the test area for the experiments at Busted Butte was not isolated by bulkheads. The tracer tests were conducted in three stages in the following order: Phase 1A, 1B, and 2. Phase 1A examined transport across the lithologic contact between the nonwelded basal vitrophyre of the Topopah Spring Tuff (Tptpv1) and the uppermost unit of the Calico Hills Formation (Tac). Phase 1B was slightly higher in the stratigraphic section; it was located entirely within the moderately welded and fractured middle portion of the vitrophyre (Tptpv2). Phase 2 (the largest test) involved all three of the lithologies tested in Phases 1A and 1B, using 37 injection points in 4 boreholes in the moderately welded and fractured portion of the vitrophyre and 40 injection points in 4 boreholes near a fracture in the Calico Hills Formation. The Phase 1 boreholes were 2 m [6.6 ft] in length, and the Phase 2 boreholes were 8.5 to 10 m [27.9 to 32.8 ft] in length.

In the Phase 1A tracer test, a mixture of nonsorbing tracers (bromide, fluorescein, pyridone, and fluorinated benzoic acids), a sorbing tracer (lithium), and fluorescent polystyrene microspheres (an analog for colloids) was injected into two boreholes in the nonwelded lower part of the basal vitrophyre and into two boreholes in the nonwelded Calico Hills tuff, after which the test area was mined back and photographed under ultraviolet light to record the distribution of fluorescein in the rock matrix around the boreholes. Fluorescein migration from the injection borehole drilled nearest the interface between the two rock units provided the clearest indicators of transport behavior. The fluorescein spread outward in all directions from the injection point in a radial but slightly flattened pattern (i.e., more elliptical than circular in cross section), an effect that the investigators noted was perhaps in response to fine-scale bedding planes in the vitrophyre. A small fracture that passed near the injection point in the borehole had little effect on diverting the movement of the tracer, indicating that matrix flow was more influential than fracture flow in the rock. As a result of small permeability differences between the basal vitrophyre and the Calico Hills tuff, the fluorescein “ponded” at the contact between the two units, forming a thin, brightly fluorescent line.

The Phase 1B test, located stratigraphically higher in the partly welded and fractured zone of the basal vitrophyre, was designed to acquire more information about fracture–matrix interactions. The test involved injecting two horizontal boreholes with the same mixture of tracers used in Phase 1A. The injection rate was 10 mL/h [0.3 oz/h] in one borehole and 1 mL/h [0.03 oz/h] in the other. Breakthrough of all five soluble tracers was observed in a monitoring borehole under the borehole with the higher injection rate {a vertical distance of about 1 m [3.3 ft]}, but no tracers were detected under the injection borehole that had the lower injection rate.

At the conclusion of the Phase 1B tracer test, the injection and monitoring boreholes were overcored, and rock samples were analyzed. The maximum concentrations of tracers were consistently recovered near the injection point, but recovery amounts varied. Bromide and fluorinated benzoic acid, both of which are nonreactive anionic tracers, were the most abundant. Although the fluorinated benzoate tracer had been injected continuously, its concentration peaked and then declined throughout the test. DOE attributed the anomalous behavior of the tracer to some unknown process, perhaps microbial activity, that caused the fluorinated benzoate to degrade during the experiment. Recovery of the fluorescein tracer also was anomalous, with measured concentrations twice that of the injected concentration. This effect

was attributed to analytical error due to the high concentration of fluorescein used in the test. Late and low recovery of pyridone was attributed to either analytical difficulties or problems with sorption or degradation of the tracer. Lithium recovery was minimal, as expected given its affinity for soprtion, though the timing and location of its arrival also conformed to that of the bromide and fluorinated benzoate tracers.

The Phase 2 test examined the role of the natural fracture pattern in the upper, partly welded portion of the vitrophyre as a transport pathway to the nonwelded tuffs below it. An alcove was excavated perpendicular to the main drift, exposing the basal vitrophyre and the uppermost Calico Hills tuffs in an outward-facing corner (two sides) of a large {10 × 10 × 7-m [32.8 × 32.8 × 23.0-ft]} block. Six horizontal injection boreholes (four of which were used in the test) were drilled parallel to each other and at the same height into the block from the side wall of the alcove. Other horizontal boreholes were drilled as collection boreholes in the lower nonwelded part of the basal vitrophyre and in the nonwelded Calico Hills tuff. Some of these boreholes were drilled from the side wall of the alcove, where they were parallel to the injection boreholes, and others were drilled perpendicular to the injection boreholes on the other side of the block exposed in the main drift.

The injected tracer solution included the same tracers as Phases 1A and 1B, plus three additional fluorinated benzoic acids, a mixture of reactive tracers, and synthetic colloids. The Phase 2 test was initiated in three stages, using different boreholes in each stage. In the first stage, an injection rate of 1 mL/h [0.03 oz/h] was used, which is within the range of present-day infiltration rates at Yucca Mountain. In the second stage, an infiltration rate of 10 mL/h [0.3 oz/h] was used, which is at the high end of the infiltration range DOE estimated for a pluvial-climate scenario. The third and most comprehensive stage of the Phase 2 test used an infiltration rate of 50 mL/h [1.7 oz/h], which was higher than naturally expected rates but was necessary for the long travel distances and short duration of the experiment.

During the Phase 2 tracer test, three additional cores were drilled in areas of the test block that were not being sampled by other collection boreholes. At the end of tracer injections, five of the injection boreholes were overcored, and a partial mineback of the Phase 2 block was performed (Groffman, et al., 2002). The mineback identified at least one fault within the test area. One of the injection boreholes was fully contained in an ash layer in the basal vitrophyre. The pattern of fluorescein migration indicated that this layer strongly affected flow by impeding movement of tracers into the remainder of the block. Nonreactive tracer breakthrough was observed in 14 of the 15 collection boreholes, with breakthrough times scaling in an approximately linear relationship with travel distance in the Calico Hills unit. A fault that may pass between one of the collection boreholes and an injection borehole in the Topopah Spring basal vitrophyre at the back of the test block appears to have significantly delayed breakthrough of tracers.

The Busted Butte test environment did not permit any direct observations about matrix diffusion processes, because the system was dominated by matrix flow. Among the main results of the tests were the DOE conclusions that flow and transport are strongly capillary dominated in the Calico Hills Formation and in the nonwelded lower part of the Topopah Spring basal vitrophyre, as demonstrated by the spreading fluorescein distributions in the Phase 1A test, by the minimal influence of fractures in the tuff near the injection sites in the boreholes, and by observations of nonreactive tracers spreading above and lateral to the injection boreholes.

2.7 Formation of Secondary Calcite and Silica in the Unsaturated Zone, Yucca Mountain

In addition to the various infiltration and seepage experiments at Yucca Mountain, geological studies of the secondary minerals that coat some fracture footwalls and lithophysal cavity floors have provided insights about unsaturated zone flow patterns in fractures. Whelan, et al. (2002) examined calcite and amorphous silica (opal) coatings from drill cores and excavated drifts to determine when and under what flow conditions the minerals formed. The secondary mineral coatings in Yucca Mountain fractures are sparse and heterogeneously distributed, with fewer than 10 percent of possible depositional sites mineralized. Coatings occur preferentially on the footwalls of fractures and are much thinner on steeply dipping fracture surfaces than on subhorizontal ones.

These observations are consistent with unsaturated zone flow processes in which fracture flow is likely to be intermittent, as contrasted with saturated zone flow in which all surfaces of all fractures would be in persistent contact with water. At a microscopic scale, Whelan, et al. (2002) also noted that the secondary coatings on shallow-dipping fractures and on lithophysal cavity floors typically have an unusual outermost coating of thin, tabular calcite crystals, some of which are capped with knobby overgrowths of late-stage calcite overgrown with opal. The observed textures are consistent with deposition from films of water fingering down fracture walls or drawn up faces of growing crystals by surface tension and evaporated at the crystal tips. Although crystal-growth depositional mechanisms involving unsaturated zone film flow and surface tension are well established, Whelan, et al. (2002) were the first to ascribe these flow processes to fracture mineral growth at Yucca Mountain.

3 OTHER EXPERIMENTS AND FIELD STUDIES

The studies described in this section are examples of recent or widely cited investigations of unsaturated flow processes at locations besides Yucca Mountain, ranging from small-scale laboratory experiments to outcrop-scale and mountain-scale field studies. The summarized papers typically are but one part of larger collections of published work about these investigations, as documented in the individual papers and their references. Few of the experiments or field studies have examined transport processes such as matrix diffusion or other fracture–matrix interactions, but they have demonstrated that even simple, well-characterized fracture systems exhibit preferential flow patterns and scale-dependent differences in flow behavior. Because variations in the flow path and the size of wetted fracture-matrix interfaces influence the effectiveness of fracture–matrix interactions, an understanding of these processes is important in the development of conceptual models of unsaturated zone transport.

3.1 Unsaturated Flow Through a Small Fracture–Matrix Network

Wood, et al. (2004) investigated a simple, well-characterized fracture network to obtain detailed information about unsaturated flow behaviors on a scale of tens of centimeters. The experiment setup consisted of 12 limestone blocks, each with nominal dimensions of 5 × 7 × 30 cm [2 × 3 × 12 in], that were stacked on end, 4 bricks wide and 3 bricks high, to form an uncemented wall 91 cm high, 28 cm wide, and 5 cm thick [35.8 in high, 11.0 in wide, and 2.0 in thick]. The joints between the blocks represented a set of connected fractures. Asperities on the blocks were minimized with sandpaper so that the blocks fit closely together. Constant volumes of tap water, preequilibrated with crushed limestone to minimize chemical interactions with the limestone blocks, were applied to the joints at the top of the wall at a rate of 1 mL/min [0.03 oz/min]. The water was applied evenly to a fiberglass wick across the full width of each joint. At the bottom of the wall, fiberglass wicks were used to collect outflow from the vertical joints into bottles. The mass of water in the collection bottles was monitored continuously. The visible contrast between dry limestone and wet limestone was sharp, facilitating the use of photography to observe the progress of wetting fronts in the tests.

Eight experiments were conducted to evaluate the repeatability of flow under nearly identical conditions and to characterize general patterns in flow behavior. Flow generally converged to one single fracture in the bottom row of blocks, with frequent switching of flow pathways during the experiments. Fracture intersections contributed to a stop-and-start advance of water through the network, generating less frequent, larger pulses of water that accumulated steadily at the fracture intersection until the capillary barrier was overcome, then advanced rapidly to the next intersection. Despite very similar initial moisture and boundary conditions, wetting front patterns in the eight experiments were less repeatable than the investigators expected.

Wood, et al. (2004) concluded that one of the more significant test observations was that slowly flowing water tended to accumulate steadily behind capillary barriers at fracture intersections until it was released rapidly as an intermittent, high-volume pulse. They also noted that some of the water that accumulated at the fracture intersections was diverted temporarily into horizontal fractures. This increased the amount of water that was pooled at the fracture intersection relative to what could be accumulated behind a capillary barrier in the vertical fracture alone.

According to Wood, et al. (2004), if the observed flow behaviors correlate with unsaturated flow mechanisms at a similar scale in natural fractured rock, they may contribute to localized fast flow paths in which slow, downward-moving flow might accumulate at fracture network intersections, then discharge abruptly in a fluid cascade. Drift- or mountain-scale flow models would not reflect the small-scale dynamics of this flow behavior, because the greater distances would tend to average out local irregularities in flow processes. However, the pattern of water movement at the scale of individual fractures could have implications in a conceptual transport model because the rapid, intermittent cascade of water would provide fewer opportunities for fracture–matrix interaction.

3.2 Unsaturated Flow Through a Fracture–Matrix Network: Dynamic Preferential Pathways in Mesoscale Laboratory Experiments

Glass, et al. (2002) conducted two sets of experiments in which water was supplied to the top of an initially dry, uncemented wall made of porous precast concrete bricks with dimensions of 5.7 × 8.9 × 19.0 cm [2.2 × 3.5 × 7.5 in] and a porosity of 0.35. The bricks were scraped to remove surface irregularities from the casting process and were stacked snugly in a simple load frame to form an uncemented brick wall. The first set of experiments used a wall that was 5.7 cm thick, 98 cm wide, and 171 cm tall [2.2 in thick, 38.5 in wide, and 67.3 in tall], forming 10 parallel vertical joints intersected by 9 parallel horizontal joints inside the wall. In the second set of experiments, the height of the wall was increased to 228 cm [90 in] by using 3 more rows of bricks, creating 3 additional sets of horizontal joints. A peristaltic pump supplied water to the network through a needle inserted into the top of one of the innermost vertical fractures. In the first experiment, a flow rate of 1.2 mL/min [0.04 oz/min] was used. In the second experiment, the entire structure was enclosed by plastic panels to inhibit evaporation, and a slightly lower flow rate of 1 mL/min [0.03 oz/min] was used. In the first experiment, the bottom of the wall acted as a capillary barrier. In the second experiment, a free-flowing boundary was created by installing fiberglass wicks at the bottom of each vertical fracture. Inflow and outflow were measured manually in the first experiment and automatically in the second experiment. The sharp visual contrast between dry concrete and wet concrete facilitated the use of photography in the first experiment, but direct observations were obscured by the plastic enclosure in the second experiment.

The first set of experiments encouraged evaporation and resulting mineral precipitation, with a wetting front that progressed in a stop-and-start pattern indicative of the fracture intersections acting as capillary barriers. Imbibition into the porous bricks from an active flow pathway was halted by capillary effects when the far side of the brick (another fracture pathway) was encountered. The flow path diverged into two pathways below the second row of bricks, but one of these two remained the primary flow pathway. Eventually a precipitate began to accumulate in the downward-flowing parts of the pathways and in the matrix. After about 39 days, the bottom part of the primary flow pathway was slowly clogged and eventually eliminated; a single fracture with wetted sides carried all the flow.

The second experiment was enclosed with a humidity barrier to minimize evaporation, and a higher wall of concrete bricks was constructed. The humidity barrier also helped to control temperature variations during the experiment. The second experiment was more complex than the first, operated for a much longer timeframe (more than 420 days), and included more

sophisticated data collection systems. In general, the pattern of outflow from the experiment showed more variability than the inflow. Clear evidence of pathway switching was observed at least five times, but in three cases, these correlated with external perturbations (e.g., changes in the inflow rates or temporary removal of the humidity barrier).

Glass, et al. (2002) observed that both experiments behaved similarly during the early stages of wetting, but evaporation and precipitation eventually dominated the flow processes in the first experiment and caused the development of starved and strengthened flow pathways. In the second experiment, the wetted structure without evaporation took on the appearance of a diffuse plume, but unsteady flow continued through the fractures. Even slight variations in ambient temperature appeared to cause switching of flow paths, perhaps in response to an evaporation–condensation mechanism. One of the unexpected results of the experiments was that preferential flow pathways evolved within the fracture network, even in the presence of strong capillary forces associated with a highly porous matrix. In the experiments, fractures demonstrated dual roles as flow conductors and as capillary barriers. Even under conditions of constant infiltration, unsaturated flow through fractured rock will create discrete pathways that are dynamic over space and time.

3.3 Experimental Studies of Water Seepage and Intermittent Flow in Unsaturated, Rough-Walled Fractures

Su, et al. (1999) conducted flow visualization experiments by using transparent epoxy casts of a natural rock fracture from the Stripa Mine, Sweden. The epoxy cast, when fitted back together, reproduced the uneven aperture surface of the natural fracture. These experiments, which did not include any matrix interactions, because the epoxy was impermeable, focused on observing the movement of infiltrating water through nonuniform, localized preferential flow paths within the fracture plane. The results of the natural-fracture experiment were compared with another set of experiments using idealized parallel plates, which also resulted in intermittent flow. The investigators noted that, even though great care was taken to maintain steady boundary conditions in these experiments, the flow was generally intermittent: threads of water along the flow channel would abruptly pinch apart, drain, and reform periodically.

The flow patterns observed in these experiments are less relevant at larger scales, where distances tend to even out the irregularities, but the shifting, localized movement of water within the single fracture is informative in terms of a conceptual model of fracture–matrix interactions. Along a preferential flow path in an unsaturated fracture, the fracture–matrix interface area is smaller and more variable than for a planar fracture as a whole.

3.4 Water Film Flow and Surface-Zone Flow Along Unsaturated Rock Fractures

In contrast to preferential flow paths observed by Wood, et al. (2004), Glass, et al. (2002), and Su, et al. (1999), various experiments by Tokunaga and Wan (2001, 1997) found that unsaturated zone fractures do not necessarily serve as capillary barriers, and water movement by film flow along a fracture surface can be rapid. Using samples of porous nonwelded Bishop Tuff, Tokunaga and Wan (1997) contrasted an aperture-based conceptual model (where water accumulates where fracture apertures are narrowest) with a model in which the fracture surface has a thin film of water over the entire surface, promoting rapid film flow during transient

high-infiltration events. Their experiment indicated that film flow was a valid mechanism capable of sustaining fast flow along truly unsaturated fractures when the partial saturation of the rock is very low. Using samples of Topopah Spring welded tuff and rhyolite from Mono County, California, Tokunaga and Wan (2001) also conducted imbibition experiments to demonstrate that more rapid flow is possible in fractured rocks where the permeability of a narrow zone adjacent to the fracture (the "fracture skin") is significantly greater than the permeability of the rock matrix as a whole, even when the rocks are at very low saturation.

3.5 Field Observation of Flow in a Fracture Intersecting Unsaturated Chalk

Infiltration tests by Dahan, et al. (1999) in the Negev Desert, Israel, were noteworthy as field-scale studies of flow processes that employed multiple sets of tracers to study flow paths *in situ* in fractured, unsaturated rock on a scale of several cubic meters. The experimental methods were similar to approaches that were also used in field studies at Yucca Mountain. The experiments involved a single natural fracture exposed to arid conditions in a large surface outcrop of low-permeability carbonate rock (chalk). The fracture was exposed in three dimensions along the top of a horizontal rock ledge and in the vertical face of the outcrop beneath the ledge. For the experiment, the horizontal ledge was cleared of unconsolidated sediments and weathered chalk, and the trace of the fracture {5.3 m [17.4 ft]} was divided by a linear grid into 21 ponded intervals. One meter below the ledge, a 25-cm [9.8-in]-diameter horizontal borehole was drilled into the rock wall along the fracture plane. Examination of the core confirmed that the entire length of the borehole {4.3 m [14.1 ft]} intersected the fracture. Seepage was monitored by a sampling apparatus, inserted into the borehole, that isolated the fracture opening into 21 separate compartments.

Flow trajectories were delineated by 7 types of fluorobenzoic acid tracers, distributed separately according to a predetermined pattern in the 21 ponded intervals on the rock ledge, and collected in the seepage trays below. The nonreactive tracers, which had similar transport behavior but could be readily distinguished chemically by their different isomers, also were determined to be unlikely to degrade under the experimental conditions.

A 5-day experiment in May 1997 was initiated by filling all of the percolation ponds with tracer-free water to a constant head of 5 cm [2.0 in] and measuring the flow rate out of each pond. Simultaneously, the seepage flow rates were measured in the borehole sampling compartments. After 43 hours, the water supply for each infiltration pond was replaced by tracer-bearing water for 6 hours, after which the supply of tracer-free water was resumed, and the experiment was continued until the concentration of tracers in the seepage dropped to zero. In a second tracer test, the tracers were applied to the infiltration ponds in a different order, so that the water percolating from each pond was tagged twice by two different tracers during two independent tests. A potential flow path between an infiltration pond and a seepage cell was delineated only where the tracers in both tests appeared in the seepage cell as well as in the infiltration pond. Further confirmation was obtained by supporting observations such as water fluxes and tracer appearances in neighboring cells.

Flow rates during the experiment varied widely, between and within cells, in the infiltration cells as well as in the seepage cells. In the early stages of the experiment, fracture infiltration rates exceeding 1,500 mL/min [51 oz/min] were observed in one cell, whereas rates less than

2 mL/min [0.06 oz/min] were observed in others. Seepage varied from more than 100 mL/min [3.4 oz/min] in some of the outlet cells to none in others. Only about 60 percent of the infiltration water was recovered as seepage. Given the low matrix permeability of the chalk formation, Dahan, et al. (1999) estimated that no more than about 2 percent of the missing water was imbibed by the matrix or retained in fracture voids, suggesting that most of the missing water percolated into the main fracture beyond the seepage collection cells or was diverted by secondary fractures along the flow path. The most important features observed in the experiment were flow instability over a 1-m [3.28-ft] interval in the fracture and the channeling of water into relatively small flow zones. Flow path delineation using tracer combinations showed that the flow channels did not always use the shortest (vertical) distance, and diagonal pathways across the fracture void were common.

3.6 Geometry and Physics of Water Flow in Fractured, Unsaturated Basalt

Layered, jointed basalt flows at the Box Canyon site in the Snake River Plain of eastern Idaho were the subject of infiltration tests conducted by the Idaho National Engineering and Environmental Laboratory (Faybishenko, et al., 2000). In an initial test in 1994 to characterize water flow in fractures on the scale of several hundred meters, a 26,000-m^2 [6.4-acre] infiltration basin was flooded with water for 36 days. After the first 6 days, tracers were added to the water. The pretest conceptual model for the basalt assumed that vertical fractures within individual basalt layers would contribute little to water movement, and most transport would occur laterally in permeable horizontal rubble zones that separated individual basalt flow. The movement of tracers through the system was studied by 101 monitoring locations, a large fraction of which were boreholes drilled away from the infiltration pond to observe the lateral migration. Contrary to expectations, however, water and tracers were not detected outside the footprint of the infiltration pond, except for a few perched water zones just above a sedimentary interbed.

The contradiction between the field observations and the original conceptual model led Faybishenko, et al. (2000) to a revised interpretation of the role played by the vertical intrabasalt fractures in controlling the spatial and temporal movement of water. Heterogeneous breakthrough curves indicated that the detection of a tracer depended strongly on the location of a sampling point and the connectivity of fractures supplying water to that point. For example, although the test was initiated with tracer-free water for 6 days, the first water to appear in several wells already contained the tracer. Conversely, in several other monitoring wells, tracer-free water was observed throughout the duration of the test.

Additional infiltration tests and modeling by Faybishenko, et al. (2000) focused on intermediate-scale (several meters) studies that examined the central portion of a single basalt flow exposed at the surface. Tracer-bearing water was supplied to a 56-m^2 [0.01-acre] pond on the outcrop during a series of 4 infiltration tests. At this smaller scale, the internal pattern of interconnected fractures within the basalt layer was found to be a major factor affecting flow. Infiltration was primarily controlled by the fracture characteristics, leading to irregular, strongly preferential, and nonrepeatable flow patterns. Fractures that were saturated early in the tests in some cases became desaturated afterwards, indicating a redistribution of water between fractures and the rock matrix.

Faybishenko, et al. (2000) developed a conceptual model in which the main processes of water flow were preferential flow through vertical fractures, fracture-to-matrix diffusion, vesicular basalt to massive basalt diffusion, a funneling effect, and some lateral flow through subhorizontal fractures and rubble zones. In this model, rapid preferential flow occurred through the largest vertical fractures, followed by a gradual wetting of other fractures and the rock matrix.

3.7 Preferential Flow of Water Through Fractured, Unsaturated Tuff at Apache Leap, Arizona

The partially welded tuff at the Apache Leap Research Site near Superior, Arizona, has been the focus of detailed hydrogeological studies. This site, along with the Peña Blanca natural analog in Mexico (Pearcy, et al., 1995), is one of the few localities besides Yucca Mountain where field studies of fracture–matrix interaction have been conducted in unsaturated volcanic tuffs. The Apache Leap Research Site is located on a mountainside in the Apache Leap Tuff, a Miocene ash flow that rests unconformably on a Paleozoic limestone surface. The tuff is extensively fractured from cooling and tectonic activity and is composed of an undetermined number of flows that occurred in rapid succession and cooled as a single unit. The basal tuff is nonwelded and grades upward into partially to densely welded tuff in the intermediate section. The top of the formation varies from partially nonwelded to nonwelded tuff. Copper is mined from the limestone that underlies the tuff, and a horizontal haulage tunnel has been cut through the tuff to connect the surface operations in the nearby town of Superior, Arizona, with the primary vertical access shaft on the east side of Apache Leap.

Davidson, et al. (1998) used geochemical and isotopic data from rock cores and water samples to evaluate the importance of fracture flow relative to matrix flow throughout the unsaturated zone over a vertical thickness of approximately 150 m [492 ft]. Data were obtained by drilling a deep-slanted borehole into the tuff from an ephemeral streambed in which infiltration was focused along fractures during rainfall events. The borehole was airdrilled and cored at a nominal dip of 45° from horizontal along a bearing that roughly paralleled the trace of the ephemeral stream. The static water level was encountered in the tuff at a vertical depth of 147 m [482 ft] below the surface, and the borehole was completed in saturated tuff at a depth of 157 m [515 ft]. Water content was measured in the core samples and by geophysical logging in the borehole. Although water flowing from a fracture was noted only at one location along the borehole, variations in water content suggested that water traveled intermittently through a number of fractures at the site. Core intervals associated with fractures were collected for isotopic analysis of their porewaters, and the sampled compositions were compared with water samples from the saturated zone. The study focused on the environmental tracers C-14 and tritium, assuming that small amounts of these radioactive tracers would diffuse into the adjacent matrix porewater during transport in fractures. If matrix flow in the rock was more important than fracture flow, a more widespread distribution of these isotopes would be expected.

Based on the analysis of the geochemical and isotopic characteristics of porewater and saturated zone water samples and supporting aqueous chemical modeling studies, Davidson, et al. (1998) concluded that at least 87 percent of the water traveled by fracture flow, not in the matrix, in the unsaturated zone. The travel time from the surface to the water table could not be estimated precisely, but the C-14 data indicated that along at least one flow path, water had

reached the saturated zone within 50 years. However, fast flow paths were not widespread. For example, sulfur isotopes suggested that most of the water in the saturated zone was older, having recharged prior to 1924 when nearby mining smelter operations increased the concentration of sulfate in the local surface environment and altered the stable isotope ratio of sulfur in recharge waters.

The study by Davidson, et al. (1998) is significant in that it examined fracture flow processes in a natural system over an extensive scale, both spatially and temporally. It is one of the few unsaturated zone field studies that has examined fracture–matrix interactions at a scale comparable to the ambient, mountain-scale flow and transport models at Yucca Mountain. Although initial values are poorly constrained in complex natural systems, Davidson, et al. (1998) used the environmental tracers analyzed in this study to suggest that fracture–matrix interactions were not extensive.

4 CONCLUSION

Tracers and dyes have been used in unsaturated zone field experiments to identify flow paths and fracture networks on a scale of several meters in fractured rocks, and some of these test data have been interpreted in the context of fracture–matrix interactions. For example, nonreactive tracers in tests at Yucca Mountain were observed to arrive late or at less than full relative concentration—an effect that could have been caused by matrix diffusion, imbibition, or diversion of some of the tracer from the main fracture flow pathway to a less conductive fracture network. In a different hydrogeological environment where matrix flow dominated over fracture flow, tracer and dye tests in the nonwelded Paintbrush Tuff and in the nonwelded Calico Hills unit at Busted Butte found few indicators of fracture–matrix interactions because of the porous, permeable nature of the matrix.

More detailed tracer experiments in Alcove 8–Niche 3 at Yucca Mountain tested for fracture-matrix interactions by injecting multiple nonreactive tracers with different molecular sizes into flowing fractures, and infiltration experiments in Alcove 6 used multiple nonreactive tracers to delineate primary and secondary flow paths. For tracers with different molecular sizes, the investigators attributed differences in breakthrough times and in relative concentrations to matrix diffusion. DOE used the results to develop and test numerical models of unsaturated zone transport. DOE conducted another major fracture–matrix interaction experiment in Alcove 8–Niche 3, the large-plot infiltration test, but variations in infiltration and seepage patterns and very low (if any) recoveries of injected tracers hindered the interpretation of test results by numerical transport simulations. The delayed and poor recoveries of tracers were cited by the investigators as possible indications that either the effective matrix diffusion coefficient is much larger and scale dependent than expected or that a larger set of conductive fractures was present, which increased the effective interface area for fracture–matrix interactions and allowed more matrix diffusion to occur.

Other unsaturated flow studies in fracture networks, including infiltration tests in a fractured chalk outcrop in Israel, dye penetration and fracture mineralization studies in welded tuffs at Yucca Mountain, and various laboratory experiments that delineated flow paths along natural or replicated fracture surfaces, have provided insights about unsaturated zone flow processes on a scale of centimeters or a few meters. The studies documented complex development of flow paths in response to subtle changes in environmental conditions (e.g., humidity and room temperature) and different infiltration rates. The tests also documented dynamic irregularities in flow paths and observations of flow path switching, fingering flow, and film flow. In the field study at Apache Leap, where the unsaturated zone of interest covered a much larger volume of rock, the details of the flow system were less apparent. Isotopic differences in matrix porewater and saturated-zone water at Apache Leap provided some evidence for fracture–matrix interactions, but the data were used mainly to establish the overall importance of fracture flow rather than matrix flow in the unsaturated tuffs.

Field experiments to quantify the importance of matrix diffusion in fractured tuffs have been challenged by some of the inherent difficulties in constraining test variables and interpreting results in a heterogeneous natural system. For example, delayed breakthrough and reduced concentrations of tracers in fracture–infiltration field tests at Yucca Mountain were attributed specifically to the process of matrix diffusion, and DOE used the test results to test numerical models in which matrix diffusion slows the transport of radionuclides. However, tests were not repeated to acquire additional data, and other factors (e.g., flow path switching, ventilation

effects, imbibition, partial sorption or degradation of tracers, or analytical errors in measuring concentrations) that were not controlled or addressed in the interpretation of the experiments may have influenced the results more than matrix diffusion.

Despite the limited number of field and laboratory studies of matrix diffusion and related fracture–matrix interactions, the cumulative results suggest that the modeling of unsaturated-zone transport processes is more dependent conceptually on small-scale flow processes than are the flow models to which transport commonly is coupled. In the development of large-scale hydrogeological models, small-scale fracture networks and heterogeneities in flow processes typically are neglected for simplicity, on the assumption that the variations average out as the scale of the system increases. The authors of a number of the papers in this overview (e.g., Salve, 2005; Salve, et al., 2002; Liu, et al., 2003; Wood, et al., 2004; Tokunaga and Wan, 2001) noted that the results of their studies suggest that conceptual models for unsaturated zone transport should be defined at a finer scale than flow models, given that small, interconnected fractures and low water fluxes in fractures are likely to enhance fracture–matrix interactions and contribute to the storage capacity of the rock. Conversely, the flow patterns observed in the concrete brick experiments by Glass, et al. (2002) could be interpreted to indicate that flow paths tend to converge, not diverge, as the scale increases. If so, fewer and fewer active fractures would carry the water, reducing the overall effectiveness of fracture–matrix interactions in slowing the transport of contaminants.

The studies summarized in this overview highlight some of the insights to conceptual models that field tests and laboratory experiments have provided about relationships between infiltration rates and flow paths in fractured, unsaturated media. Outcomes of many of the studies also have highlighted the practical difficulties in quantifying fracture–matrix interactions in the heterogeneous subsurface at Yucca Mountain, such that a range of uncertainties apply to site-scale unsaturated zone transport models. Given these complexities, it is important that a model of unsaturated zone transport for a potential repository include consideration of the full range of data and model uncertainties for the parameters that are used to represent fracture–matrix interactions.

5 REFERENCES

Arnon, S., E. Adar, Z. Ronen, A. Yakirevich, and R. Nativ. "Impact of Microbial Activity on the Hydraulic Properties of Fractured Chalk." *Journal of Contaminant Hydrology*. Vol. 76. pp. 315–336. 2005.

Bechtel SAIC Company, LLC. "Analysis of Alcove 8/Niche 3 Flow and Transport Tests." ANL–NBS–HS–000056. Rev 00. Las Vegas, Nevada: Bechtel SAIC Company, LLC. 2006.

———. "*In-Situ* Field Testing of Processes." ANL–NBS–HS–000005. Rev 02. Las Vegas, Nevada: Bechtel SAIC Company, LLC. 2004a.

———. "Technical Basis Document No. 10: Unsaturated Zone Transport." Rev 01. Las Vegas, Nevada: Bechtel SAIC Company, LLC. 2004b.

———. "Technical Basis Document No. 3: Water Seeping into Drifts." Rev 02. Las Vegas, Nevada: Bechtel SAIC Company, LLC. 2004c.

———. "Total System Performance Assessment–License Application Methods and Approach." TDR–WIS–PA–000001. Rev 00 ICN 01. Las Vegas, Nevada: Bechtel SAIC Company, LLC. 2003.

———. "Analysis of Geochemical Data for the Unsaturated Zone." ANL–NBS–HS–000017. Rev 00 ICN 02. Las Vegas, Nevada: Bechtel SAIC Company, LLC. 2002.

———. "Unsaturated Zone and Saturated Zone Transport Properties (U0100)." ANL–NBS–HS–000019. Rev 00 ICN 02. Las Vegas, Nevada: Bechtel SAIC Company, LLC. 2001.

Dahan, O., R. Nativ, E.M. Adar, B. Berkowitz, and Z. Ronen. "Field Observation of Flow in a Fracture Intersecting Unsaturated Chalk." *Water Resources Research*. Vol. 35. pp. 3,315–3,326. 1999.

Davidson, G.R., R.L. Bassett, E.L. Hardin, and D.L. Thompson. "Geochemical Evidence of Preferential Flow of Water Through Fractures in Unsaturated Tuff, Apache Leap, Arizona." *Applied Geochemistry*. Vol. 13. pp. 185–195. 1998.

Faybishenko, B., C. Doughty, M. Steiger, J.C.S. Long, T.R. Wood, J.S. Jacobsen, J. Lore, and P.T. Zawislanski. "Conceptual Model of the Geometry and Physics of Water Flow in a Fractured Basalt Vadose Zone." *Water Resources Research*. Vol. 36. pp. 3,499–3,520. 2000.

Glass, R.J., M.J. Nicholl, S.E. Pringle, and T.R. Wood. "Unsaturated Flow Through a Fracture-Matrix Network: Dynamic Preferential Pathways in Mesoscale Laboratory Experiments." *Water Resources Research*. Vol. 38. p. 1,281. doi:10.1029/2001WR001002. 2002.

Groffman, A.R., H.J. Turin, M.A. McGraw, C.L. Jones, C.D. Scism, and W.E. Soll. "Busted Butte Phase 2: Analysis of Post-Test Mineback and Overcore Rock Samples." Geological Scoiety of America Abstracts with Programs. No. 34, Abstract 45930. Boulder, Colorado: Geological Society of America. 2002.

Hinds, J.J., G.S. Bodvarsson, and G.H. Nieder-Westermann. "Conceptual Evaluation of the Potential Role of Fractures in Unsaturated Processes at Yucca Mountain." *Journal of Contaminant Hydrology*. Vols. 62–63. pp. 111–132. 2003.

Hu, Q., T.J. Kneafsey, R.C. Trautz, and J.S.Y. Wang. "Tracer Penetration into Welded Tuff Matrix from Flowing Fractures." *Vadose Zone Journal*. Vol. 1. pp. 102–112. 2002.

Hu, Q., R. Salve, W.T. Stringfellow, and J.S.Y. Wang. "Field Tracer-Transport Tests in Unsaturated Fractured Tuff." *Journal of Contaminant Hydrology*. Vol. 51. pp. 1–12. 2001.

Jakob, A. "Matrix Diffusion for Performance Assessment–Experimental Evidence, Modeling Assumptions and Open Issues." PSI Bericht No. 04-08. Switzerland: Paul Scherrer Institute. 2004.

Liu, H-H., C.B. Haukwa, C.F. Ahlers, G.S. Bodvarsson, A.L. Flint, and W.B. Guertal. "Modeling Flow and Transport in Unsaturated Fractured Rock: An Evaluation of the Continuum Approach." *Journal of Contaminant Hydrology*. Vol. 62–63. pp. 173–188. 2003.

Liu, H.H., C. Doughty, and G.S. Bodvarsson. "An Active Fracture Model for Unsaturated Flow and Transport in Fractured Rocks." *Water Resources Research*. Vol. 34. pp. 2,633–2,646. 1998.

NRC. "Resolution of KTIs for High-Level Waste Disposal." 2007. <http://www.nrc.gov/waste/hlw-disposal/reg-initiatives/resolve-key-tech-issues.html> (09 August 2007).

Pearcy, E.C., J.D. Prikryl, and B.W. Leslie. "Uranium Transport Through Fractured Silicic Tuff and Relative Retention in Areas with Distinct Fracture Characteristics." *Applied Geochemistry*. Vol. 10. pp. 685–704. 1995.

Salve, R. "Observations of Preferential Flow During a Liquid Release Experiment in Fractured Welded Tuffs." *Water Resources Research*. Vol. 41. W09427, doi:10.1029/2004WR003570. 2005.

Salve, R., H-H. Liu, P. Cook, A. Czarnomski, Q. Hu, and D. Hudson. "Unsaturated Flow and Transport Through a Fault Embedded in Fractured Welded Tuff." *Water Resources Research*. Vol. 40. W04210, doi:10.1029/2003WR002571. 2004.

Salve, R., C.M. Oldenburg, and J.S.Y. Wang. "Fault-Matrix Interactions in Nonwelded Tuff of the Paintbrush Group at Yucca Mountain." *Journal of Contaminant Hydrology*. Vols. 62–63. pp. 269–286. 2003.

Salve, R., J.S.Y. Wang, and C. Doughty. "Liquid-Release Tests in Unsaturated Fractured Welded Tuffs: I. Field Investigations." *Journal of Hydrology*. Vol. 256. pp. 60–79. 2002.

Su, G.W., J.T. Geller, K. Pruess, and F. Wen. "Experimental Studies of Water Seepage and Intermittent Flow in Unsaturated, Rough-Walled Fractures." *Water Resources Research*. Vol. 35. pp. 1,019–1,037. 1999.

Tokunaga, T.K. and J. Wan. "Surface-Zone Flow Along Unsaturated Rock Fractures." *Water Resources Research*. Vol. 37. pp. 287–296. 2001.

———. "Water Film Flow Along Fracture Surfaces of Porous Rock." *Water Resources Research*. Vol. 33. pp. 1,287–1,295. 1997.

Weisbrod, N., O. Dahan, and E.M. Adar. "Particle Transport in Unsaturated Fractured Chalk Under Arid Conditions." *Journal of Contaminant Hydrology*. Vol. 56. pp. 117–136. 2002.

Whelan, J.F., J.B. Paces, and Z.E. Peterman. "Physical and Stable-Isotope Evidence for Formation of Secondary Calcite and Silica in the Unsatured Zone, Yucca Mountain, Nevada." *Applied Geochemistry*. Vol 17. pp. 735–750. 2002.

Wood, T.R., R.J. Glass, T.R. McJunkin, R.K. Podgorney, R.A. Laviolette, K.S. Noah, D.L. Stoner, R.C. Starr, and K. Baker. "Unsaturated Flow Through a Small Fracture–Matrix Network: Part 1. Experimental Observations." *Vadose Zone Journal*. Vol. 3. pp. 90–100. 2004.

Zhou, Q., R. Salve, H-H. Liu, J.S.Y. Wang, and D. Hudson. "Analysis of a Mesoscale Infiltration and Water Seepage Test in Unsaturated Fractured Rock: Spatial Variabilities and Discrete Fracture Patterns." *Journal of Contaminant Hydrology*. Vol. 87. pp. 96–122. 2006.